

On-site Hydrogen Peroxide Production at Pilot Flow Plant: Application to Electro-Fenton Process

Eloy Isarain-Chávez¹, Catalina de la Rosa¹, Carlos A. Martínez-Huitle², Juan M. Peralta-Hernández^{1,*}

¹Centro de Innovación Aplicada en Tecnologías Competitivas (CIATEC), Departamento de Investigación Ambiental Omega-201, Fraccionamiento Industrial Delta. León, 37545, Guanajuato, México

²Universidade Federal do Rio Grande do Norte, Instituto de Química, Lagoa Nova CEP 59078-970 - Natal, RN, Brazil

*E-mail: jperalta@ciatec.mx

Received: 2 January 2013 / Accepted: 13 February 2013 / Published: 1 March 2013

In recent years, the in situ electrochemical generation of the Fenton reagent, also known as the electro-Fenton (EF) approach, has been studied in order to achievement the fact that the reduction of dissolved oxygen to hydrogen peroxide (H₂O₂) can be carried out selectively in acidic medium. This work describes the results obtained in the low flow plant (V = 3 L) with a boron doped diamond (BDD) as a cathode operating at constant current density, room temperature and liquid flow rate of 12 L min⁻¹, employed for on-site H₂O₂ production in acidic medium (pH 3) to promote EF treatment. These processes were evaluated by their abilities to degrade a commercial methyl orange (MO) azo dye. Small quantities of generated carboxylic acids like ascorbic, benzoic, citric, maleic and oxalic acid were detected by HPLC determinations. Based on the use of a BDD cathode, is possible the effectively production of H₂O₂ in the medium via oxygen reduction. The dye MO was quickly removed during the first minutes of the treatment, yielding closely 80% of decolorization efficiency under optimized conditions and 7.66 kWh m⁻³ energy consumption. HPLC analysis confirmed that the MO degradation became effective.

Keywords: Azo dye, Carboxylic acids, Electro-Fenton, Hydrogen peroxide, Waste water treatment

1. INTRODUCTION

Hydrogen peroxide (H₂O₂) is currently one the most common chemicals used for water treatment and chemical production, and it is a promising oxidant for green chemistry processes in the near future [1]. The use of H₂O₂ may offer an efficient alternative for controlling pollution in aqueous media. Hydrogen peroxide is one the most popular non-selective oxidizing agents that are used to convert organic compounds to carbon dioxide [2]. Several works have demonstrated that on-site

electrochemical generation of H_2O_2 can be used successfully to decontaminate effluents with different organic compounds [3-6]. In this process, H_2O_2 is continuously supplied to the contaminated solution through oxygen (O_2) reduction by two electrons in an acidic medium, according to the following equation [7-12]:



The most common use of H_2O_2 in environmental applications involves the addition of iron (Fe^{2+}) to the acidic solution to increase the oxidizing power of the H_2O_2 by forming hydroxyl radicals ($\bullet OH$) via the Fenton's reaction, according to the equation [10,13-14]:



This method is commonly referred to as electro-Fenton (EF) treatment and is considered an advanced oxidation process (AOP) [15]. The principal reason for combining on-site hydrogen peroxide generation and the Fenton's reaction is to improve the oxidation capacities of the two individual processes, creating a synergetic system [16]. The hydroxyl radical species that are produced through these processes are characterized by a large oxidation power (2.8 V vs ENH) [17] that is able to transform organic compounds into CO_2 and H_2O [18].

The aim of this work is to present the effectiveness of these water-treatment processes by studying the degradation of the azo dye Methyl Orange (MO). Tests were carried out using a continuous flow reactor $V = 3L$ that was operated to produce on-site H_2O_2 using the Electro-Fenton processes. Although, the effectiveness of these AOPs is almost definitive, maybe, these technologies can be considered feasible for treating wastewaters containing dyes, if the by-products during electrochemical treatment are monitored and studied. Therefore, using HPLC measurements, several metabolites were identified and quantified, such as ascorbic, benzoic, citric, maleic and oxalic acid.

2. EXPERIMENTAL DETAILS.

The chemicals used in this work, such as sulfuric acid (H_2SO_4), sodium sulfate (Na_2SO_4), and ferrous sulfate ($FeSO_4 \cdot 7H_2O$), were purchased from J.T. Baker as ACS reagent grade and were used as received, without further purification. Titanium (IV) oxysulfate ($TiOSO_4$, 99.99%, ca. 15 wt. diluted sulfuric acid solution) and the azo dye Methyl Orange ($C_{14}H_{14}N_3NaO_3S$, dye content 85 %) were purchased from Sigma-Aldrich.

2.1. Electrochemical flow reactor.

Figure 1 shows a sketch of the recirculation flow plant with a one-compartment filter-press reactor used for Methyl Orange (MO) degradation. For each trial, 3 L of solution were introduced into

the reservoir and recirculated through the system by a magnetic drive centrifugal pump at a flow rate of 12 L min^{-1} regulated by a rotameter. The electrochemical reactor contained a BDD/BDD as anode and cathode. Both electrodes were rectangular plates with a geometric area of 64 cm^2 in contact with the solution, and separated a distance of 2.5 cm. The BDD electrode with a thickness of 2-7 μm supported on niobe was provided by MetakemTM. All electrolyses were performed at constant applied current density (j_{appl}) supplied by a BK Precision DC Regulated power supply. Prior to the degradation experiments, a 0.05 M Na_2SO_4 solution was electrolyzed in the plant at 50 mA cm^{-2} for 60 min to remove the impurities of the BDD surface [10,19].

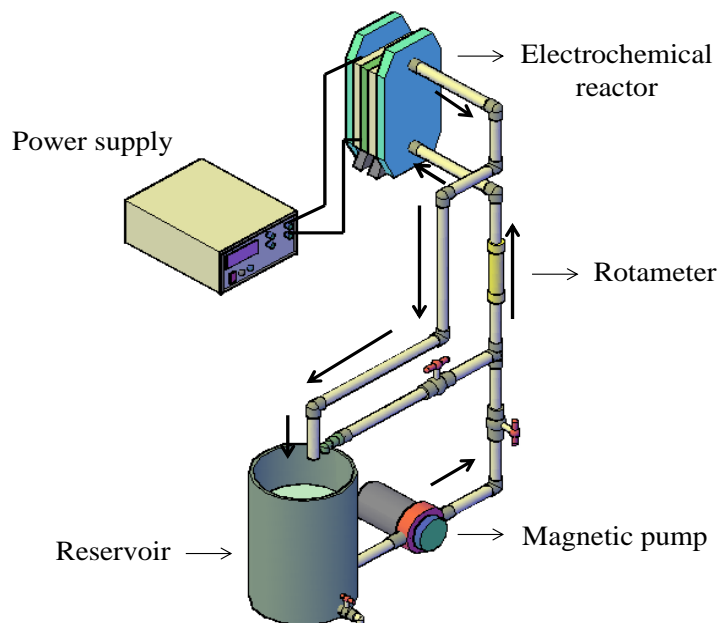


Figure 1. Sketch of the experimental set-up used for the degradation of Methyl Orange by electro-Fenton (EF) processes using a two-electrode with monopolar connection. The anodes and cathodes were of boron-doped diamond (BDD) thin film.

Solutions with MO were prepared at different concentration ranging from 50 to 250 mg L^{-1} were comparatively degraded in 0.05 M Na_2SO_4 as background electrolyte at different j_{appl} (7.8 and 31 mA cm^{-2}) at ambient temperature ($25 \pm 1 \text{ }^\circ\text{C}$) for 60 min as limit time. The dye concentrations were chosen since they are typical values in industrial textile wastewaters [10].

2.2. Evaluation on-site H_2O_2 production.

Electrolysis experiments were carried out to test the capacity of the reactor to produce H_2O_2 through the cathodic reduction of dissolved O_2 . The pH of dye solutions was initially adjusted with H_2SO_4 to 3.0 and was not further regulated since it slightly decayed up to a value of 2.7-2.8 as maximal during the treatments. The concentration of H_2O_2 generated during electrolysis was

determined by titrating with titanium (IV) oxysulfate and measuring the intensity of the color of the H_2O_2 reagent complex at a wavelength of 406 nm [19].

2.3. MO solution preparation

An accurately weighed quantity of the MO dye was dissolved in distilled water to prepare a stock solution (1000 mg L^{-1}), and experimental solutions of the desired concentration (100 , 150 and 200 mg L^{-1}) were obtained by successive dilution. The synthetic textile dye wastewater solution was prepared in accordance with previous reports [20,21] in which dye concentrations ranged between 10 and 200 mg L^{-1} .

2.4. Analytical procedure.

The absorbance decay ($\lambda_{\text{max}} = 506 \text{ nm}$) for treated dye solutions was monitored from the spectra measured between 300 and 800 nm at certain time intervals using a Thermo Scientific 300-UV, UV-Vis spectrophotometer. Generated carboxylic acids were detected and quantified by HPLC analysis with an Agilent 1100 LC equipped with an Agilent 1100 Series UV/vis detector set at $\lambda = 210 \text{ nm}$. The LC was filled with a Luna 5u C-18 ($150 \text{ mm} \times 4.6 \text{ mm}$, $5 \mu\text{m}$) column at $30 \text{ }^\circ\text{C}$. For these analyses, $20 \mu\text{L}$ samples were injected into the LC and a 25 mM potassium dihydrogenphosphate solution of $\text{pH } 2.5$ (adjusted with phosphoric acid) at 1.3 mL min^{-1} was circulated as mobile phase.

3. RESULTS AND DISCUSSION.

3.1. Electrochemical generation of H_2O_2 in the flow reactor.

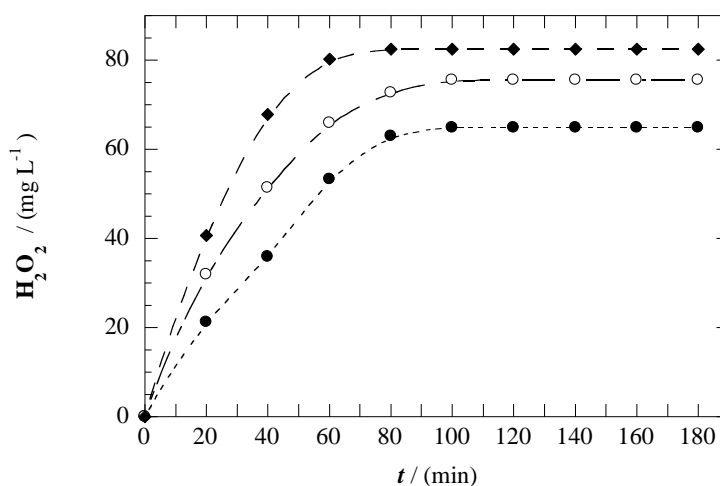


Figure 2. Time-course evolution of the concentration of H_2O_2 during the electrolysis of 3 L solutions containing $0.05\text{M Na}_2\text{SO}_4$ at $\text{pH } 3.0$ and $25 \text{ }^\circ\text{C}$. With a flow rate of 12 L min^{-1} and a current density of: (●) 7.8 mA cm^{-2} , (○) 15 mA cm^{-2} and (◆) 31 mA cm^{-2} .

Several tests were performed to evaluate the electrochemically generated H_2O_2 concentration in the flow reactor at different current densities (j). The capacity of the system to electrochemically generate H_2O_2 at the BDD cathode through O_2 reduction (Eq. 1) was studied spectrophotometrically [19]. Figure 2 shows the variation of the H_2O_2 concentration as a function of the electrolysis time and current densities and flow rate $Q = 12 \text{ L min}^{-1}$. Curve (\bullet) corresponds to a sample in which the current density was 7.8 mA cm^{-2} ; in this case, the H_2O_2 concentration was approximately 64 mg L^{-1} after a reaction time of 180 min. Curve (\circ) corresponds to a current density of 15 mA cm^{-2} , and the resulting H_2O_2 accumulation was approximately 72 mg L^{-1} after 180 min of electrolysis. Finally, curve (\blacklozenge) shows a current density of 31 mA cm^{-2} , which resulted in $82 \text{ mg L}^{-1} \text{ H}_2\text{O}_2$.

In all cases, it can be seen that the H_2O_2 concentration is proportional to the current density supplied to the system. On the other hand, the H_2O_2 concentration did not increase linearly with reaction time; after about 80 min, the H_2O_2 concentration reached its steady-state value and remained almost constant for the remainder of the reaction time. From these results, it is apparent that H_2O_2 undergoes chemical decomposition O_2 either on the anode (heterogeneous process) or in the medium (homogeneous process) [22].

3.2. Effect of applied current densities over MO degradation under EF processes.

The decay of different concentration methyl orange during the electrolysis at different current densities ($j = 7.8, 15$ and 31 mA cm^{-2}) was followed by spectrophotometric measurements, and the results are shown in Figure 3. The absorption spectra of methyl orange at room temperature present a maximum absorption at 506 nm, which is directly related to the MO concentration and also to the color of the solution. As can be observed, increasing the current density resulted in a faster decolorization of the solution. In this electrochemical technique, pollutants are mainly destroyed by the action of $\bullet\text{OH}$ formed as intermediate at the solution by means Fenton's process in accordance reaction 2 [23].

As shown, regardless of the initial concentration of dye (100, 150 or 200 mg L^{-1}), Figure 3 (a,b,c, respectively) there is a clear effect of increased oxidation power as the current densities increases, for the formation rates of active species are certainly higher at higher j_{appl} . As estimated, increasing j_{appl} resulted in a faster decolorization of MO, due to a great H_2O_2 production. As j_{appl} increases from 7.8 mA cm^{-2} to 31 mA cm^{-2} , the degradation rate is increased, being the most efficient when is applied the $j = 31 \text{ mA cm}^{-2}$. It has been reported that under constant j_{appl} , the electro-generation of H_2O_2 at BDD surface is continuous [10,19] the higher j_{appl} carry out the production of larger amount of H_2O_2 favoring the removal of organic compounds with time. Then, the appropriate choice of j_{appl} favors a more efficient degradation treatment.

3.3. Effect of MO dye concentration.

The Figure 3 also shows changes in absorbance decay over time, during electrolysis of synthetic wastes polluted with initially different MO dye concentrations. It can be observed that trends

of absorbance decay coincide and similar specific energy values are required to achieve complete waste decolorization.

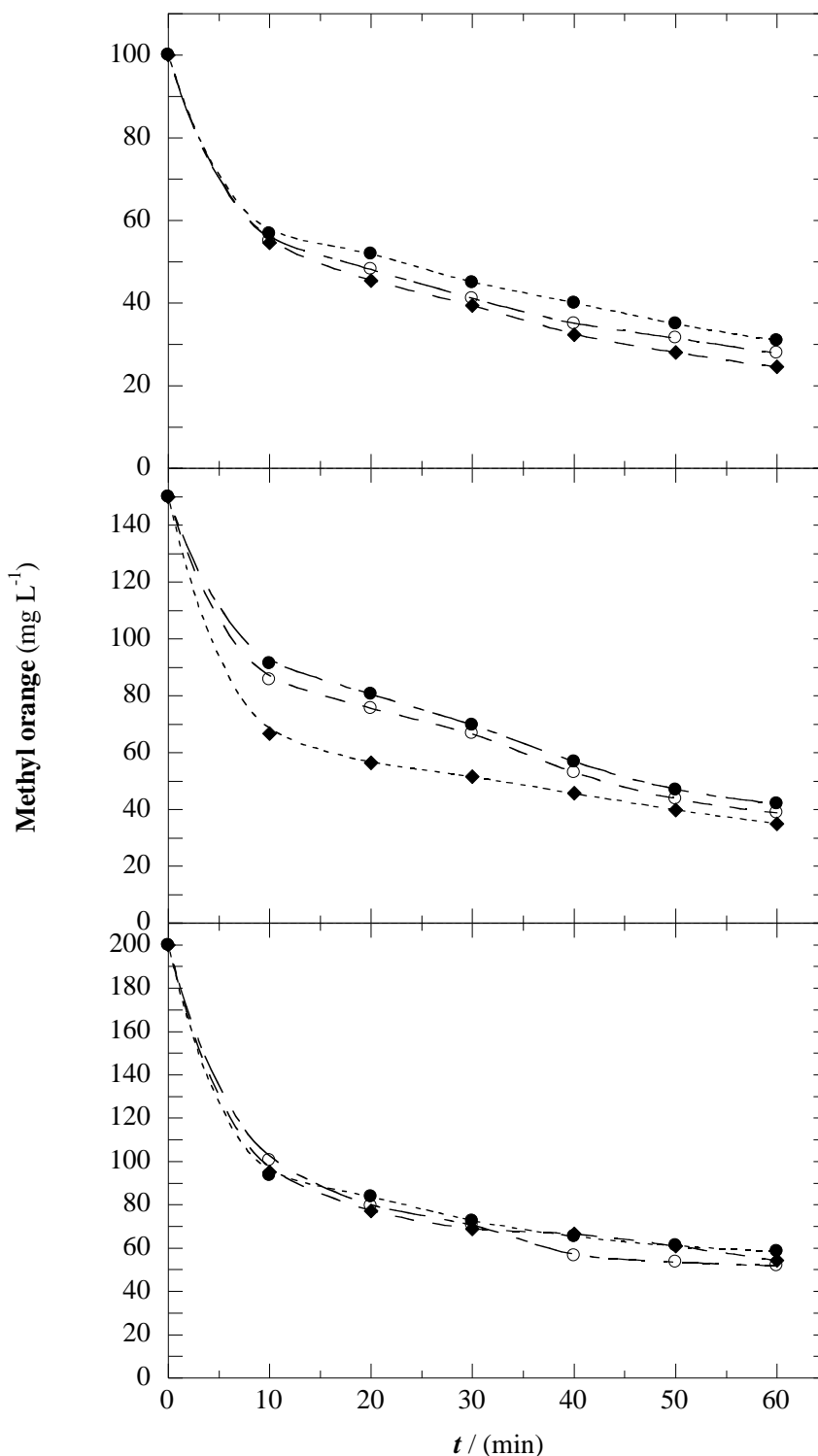


Figure 3. Effect of current on (a, b and c) removal with electrolysis time for electro-Fenton degradation of 100, 150 and 200 mg L⁻¹, of Methyl Orange solution in 0.05M Na₂SO₄ at pH 3.0 and 25 °C. With 3 L of solution, flow rate of 12 L min⁻¹ and a current density of: (●) 7.8 mA cm⁻², (○) 15 mA cm⁻² and (◆) 31 mA cm⁻².

This shows that both oxidation rate and process efficiency are directly proportional to azo dye concentration. As can be observed, for high pollutant concentrations, maximum efficiencies are obtained during initial process phases, with subsequent constant efficiency loss during the experiment. This behavior is characteristic of discontinuous electrochemical oxidation of wastewaters with electro-Fenton process.

The highest decolorization efficiency was obtained by applying 31 mA cm^{-2} and 80 mg L^{-1} of H_2O_2 . The results of Figure 3 also show that MO is quickly decolorized during the first 10 min under these conditions, yielding 80% of decolorization efficiency, whereas at the same time, the use of 7.8 and 15 mA cm^{-2} lead to 70% and 60% decolorization efficiency, respectively.

3.4. Determination of kinetic decolorization.

The decolorization kinetics of MO by electro-Fenton was studied for various contact times. The data were then regressed for the pseudo-first order kinetic equation (3); [24]. The calculated kinetic parameters were presented in Table 1.

$$\frac{1}{A_t} = \frac{1}{A_0} + k_2 t \quad (3)$$

where A_0 is initial absorbance of the dye, A_t is effluent absorbance of the dye at time t , and k_2 ($\text{A}^{-1} \text{ min}^{-1}$) are the rate constants of the pseudo first-order kinetic equation.

Table 1. Evaluation of kinetic constants for the decolorization MO by means BDD/BDD set up using equation 3.

Concentration (mg L^{-1})	j (mA cm^{-2})	k (min^{-1})	R^2
100			
	7.8	0.4272	0.9978
	15	0.5050	0.9968
	31	0.5580	0.9963
150			
	7.8	7.7252	0.9913
	15	9.1729	0.9930
	31	13.1650	0.9933
200			
	7.8	7.3786	0.9698
	15	9.4017	0.9869
	31	11.1130	0.9866

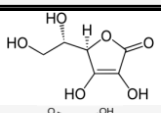
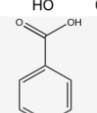
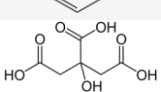
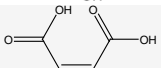
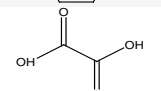
These results suggest that the best experimental conditions for the decolorization under electro-Fenton process occurred with the addition of 150 mg L⁻¹ and 200 mg L⁻¹ of MO, applying 31 mA cm⁻² and after 60 min electrolysis, as expected from the highest kinetic constant found of 13.16 min⁻¹ and 11.11 min⁻¹ under these conditions.

3.5. Identification and evolution of generated carboxylic acids

All chromatograms of electrolyzed solutions of methyl orange showed well-defined peaks associated with carboxylic acids such as oxalic ($t_r = 1.63$ min), ascorbic ($t_r = 1.94$ min), citric ($t_r = 2.93$ min), maleic ($t_r = 4.1$ min), and benzoic ($t_r = 10.36$ min), these results are shown in Table 2. Benzoic acid is expected from the dissociation of its complex with the azo dye. This acid is produced from the degradative cleavage of benzene groups such as sodium benzoate as product of reaction decarboxylation. While that of the maleic acids are produced from the degradative cleavage of benzene groups of methyl orange. Oxalic acid is ultimate acid that is mineralized to CO₂.

The citric acid was rapidly reduced by electro-Fenton processes, being eliminated between 0 and 20 min. That means that it's quickly destroyed by radicals $\bullet\text{OH}$. This behavior was observed for maleic acid, disappearing between 50 and 60 min in all cases, which for sake of simplicity are not shown. On the other hand a different trend was obtained for ascorbic acid reached 0.42 mg L⁻¹ as maximum accumulation at 40 min with current density of 7.8 mA cm⁻² and 200 mg L⁻¹ of methyl orange. This acid was very slowly mineralized and remains up to the end of electrolysis due to lower concentrations of hydroxyl radicals in the dissolution. The same trend can be observed in Fig. 4a for the same acid with 150 mg L⁻¹, accumulated in much less up to 0.15 mg L⁻¹ at 20 min, although in this case it decays slightly faster, where it practically disappears in 50 min.

Table 2. Products identified during the electro-Fenton degradation of methyl orange with 0.05M Na₂SO₄ in presence of 0.3 mM Fe²⁺ at pH 3.0, using flow cell of 3 L at 25 °C, at different times of electrolysis.

Compound	Analytical technique	Retention time (min)	Chemical structure
Ascorbic acid	HPLC	1.94	
Benzoic acid	HPLC	10.36	
Citric acid	HPLC	2.93	
Maleic acid	HPLC	4.1	
Oxalic acid	HPLC	1.63	

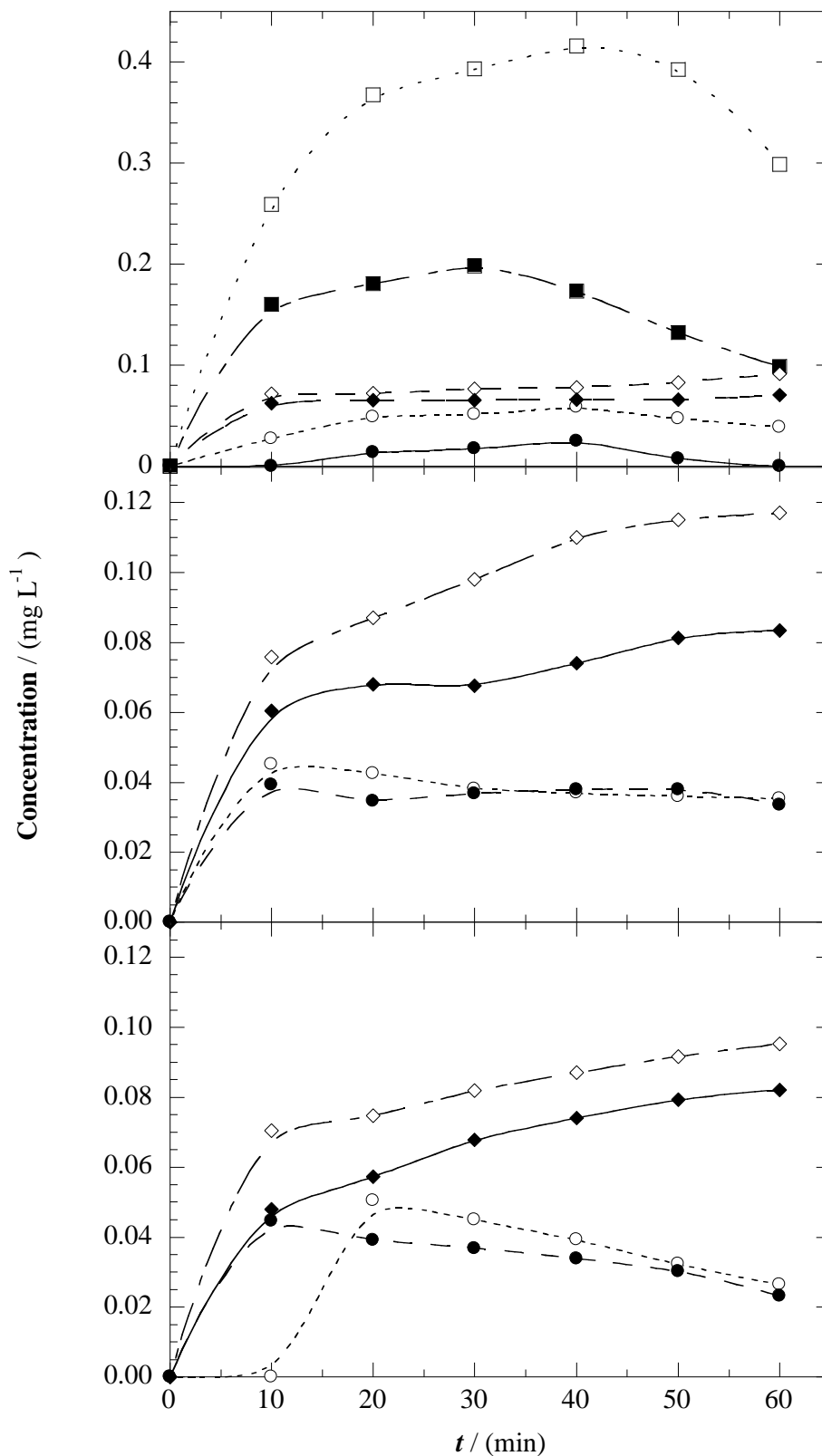


Figure 4. Evolution of the concentration of generated carboxylic acids during the treatment of Methyl Orange with 0.3 mM Fe²⁺ at pH 3.0 and 25 °C using electrochemical cell by mean of electro-Fenton process with BDD anode and cathode. Full symbols (●) with 150 mg L⁻¹, empty symbols (○) with 200 mg L⁻¹. Plot (a): 7.8 mA cm⁻², (b): 15 mA cm⁻², and (c) 31 mA cm⁻². (●,○) oxalic acid, (◆,◇) benzoic acid, and (■,□) ascorbic acid.

In contrast, maleic acid was slowly eliminated in 60 min of electrolysis with 100 mg L^{-1} , and a current density of 31 mA cm^{-2} (not shown in Fig. 4). This suggests that are more slowly oxidized with $\bullet\text{OH}$ in solution. This effect can be better discussed from the evolution of oxalic and benzoic acids.

Fig. 4b evidences a very slow removal for benzoic acid, after its maximum accumulation almost 0.12 and 0.08 mg L^{-1} at 60 min, indicating that both acids react difficultly with the amounts of BDD($\bullet\text{OH}$) and $\bullet\text{OH}$ formed at 15 mA cm^{-2} . And a similar behavior was found for this acid, as can be seen in Fig. 4c.

On the other hand the Fig. 4a, 4b and 4c shows a quite similar evolution of oxalic acid at currents density of 7.8 , 15 and 31 mA cm^{-2} in all processes. Unfortunately this acid cannot disappear, in 60 min, as expected, due to lower concentrations of radicals $\bullet\text{OH}$ generated in solution and the short time of electrolysis. This indicating that Fe(III) an Fe(II) oxalate complexes react difficultly with the amounts of BDD ($\bullet\text{OH}$) formed under these conditions.

But at current density of 31 mA cm^{-2} and 200 mg L^{-1} accelerates the destruction of this acid up to 0.025 mg L^{-1} at 60 min, as expected are more easily mineralized by higher concentration of hydroxyl radicals even though there are a more largely concentration of precedent compounds. As stated above, the enhancement of $\bullet\text{OH}$ production in BDD/BDD cell, and the presence of 0.3 mM Fe^{2+} improve the reaction of Fe(II)-oxalate and Fe(III)-oxalate complexes can be destroyed by the excess of the above oxidant.

All these findings agree with UV decays of the Methyl orange solution shown in Fig. 3a, 3b and 3c with different current density for all electrochemical processes. Thus, the best mineralization found for EF with 0.3 mM Fe^{2+} , 31 mA cm^{-2} and 200 mg L^{-1} , this phenomenon can be ascribed to the efficient oxidation of the Fe(II) complexes with the ultimate carboxylic acid like oxalic and by the great amount of $\bullet\text{OH}$ formed from Fenton's reaction (2).

4. CONCLUSIONS

The degradation of MO in acidic aqueous medium was carry out applying electro-Fenton process based on the use of a BDD/BDD system at electrochemical flow reactor, rate 12 L min^{-1} and $V = 3 \text{ L}$ and 7.66 kWh m^{-3} energy consumption. The results evidenced that the best conditions for removal 200 mg L^{-1} of MO is when we applied 31 mA cm^{-2} with 0.3 mM Fe^{2+} . Generated carboxylic acids such as ascorbic, benzoic, citric, maleic and oxalic were detected by ion-exclusion HPLC. It can be a feasible process for decolorizing wastewaters containing dyes as a pre-treatment process as a previous step to biological depuration or it could be coupled with other wastewater treatments (e. g.: UV irradiation) reducing significantly the cost and time treatment.

ACKNOWLEDGMENTS

The authors thank the CIATEC GD0059, GD0065 and FORDECyT 143288 for financial support. JMPH also acknowledges Salvador Viñals Uyà (Volunteer from Peace Corps under agreement with CONACyT) for his help in the manuscript's revision.

References

1. N. Gullet, L. Roué, S. Marcotte, D. Villers, J.P. Dodelet, N. Chim, S. Trévin, *J. Appl. Electroche*, 36 (2006) 863
2. C. Badellino, C. Arruda Rodrigues, R. Bertazzoli, , *J. Hazard. Mat*, 137 (2006) 856
3. C.A. Martínez-Huitle, E. Brillas, , *Appl. Cat. B: Environ*, 87 (2009) 105–145
4. G. Zhang, F. Yang, Mingming Gao, X. Fang, L. Liu, *Electrochim. Acta*, 53 (2008) 5155
5. M. Skoumal, R.M. Rodriguez, P. Lluís Cabot, F. Centellas, J.A. Garrido, C. Arias, E. Brillas, *Electrochim. Acta*, 54 (2009) 2077
6. J.M. Peralta-Hernández, Y. Meas-Vong, F.J. Rodríguez, T.W. Chapman, M.I. Maldonado, L.A. Godínez, *Dyes and Pigments*, 76 (2008) 656
7. E. Brillas, M.A. Baños, S. Camps, C. Arias, P-L. Cabot, J.A. Garrido, R.M. Rodríguez, *New. J. Chem.* 28 (2004) 314
8. J.M. Peralta-Hernández, C.A. Martínez-Huitle, J.L. Guzmán-Mar, A. Hernández-Ramírez, *J. Environ. Eng. Manage*, 19 (2009) 257
9. J.M. Peralta-Hernández, Y. Meas-Vong, F.J. Rodríguez, T.W. Chapman, M.I. Maldonado, L.A. Godínez, *Water Res*, 40 (2006) 1754
10. K. Cruz-González, O. Torres-López, A. García-León, J.L. Guzmán-Mar, L.H. Reyes, A. Hernández-Ramírez, J.M. Peralta-Hernández, *Chem. Eng. J*, 160 (2010) 199
11. B. Balci, N. Oturan, R. Cherrier, M.A. Oturan, *Water Res*, 43 (2009) 1924
12. A. Lahkimi, M.A. Oturan, N. Oturan, M. Chaouch, *Environ. Chem Lett*, 5 (2007) 35
13. D. Melgoza, A. Hernández-Ramírez, J.M. Peralta-Hernández, *Photochem. Photobiol. Sci.* 8 (2009) 596
14. J. Anotai, M-Ch. Lu and P. Chewprecha, *Water Res*, 40 (2006) 1841
15. K. Esquivel, L.G. Arriaga, F.J. Rodríguez, L. Martínez, L.A. Godínez, *Water Res*, 43 (2009) 3593
16. A. Özcan, M.A. Oturan, N. Oturan, Y. Sahin, *J. Hazard. Mat*, 163 (2009) 1213
17. E. Guinea, C. Arias, P. Lluís Cabot, J.A. Garrido, R.M. Rodríguez, F. Centellas, E. Brillas, *Water Res*, 42 (2008) 499
18. Y.B. Xie, X.Z. L, *Mat. Chem. Phys*, 95 (2006) 39
19. K. Cruz-González, O. Torres-López, A.M. García-León, E. Brillas, A. Hernández-Ramírez, J.M. Peralta-Hernández, *Desalination*, 286 (2012) 63
20. Y. Yavuz, R. Shahbazi, *Sep. Purif. Technol*, 85 (2012) 130
21. E.J. Ruiz, C. Arias, E. Brillas, A. Hernández-Ramírez, J.M. Peralta-Hernández, *Chemosphere*, 82 (2011) 495
22. A. Wang, J. Qu, J. Ru, H. Liu, J. Ge, *Dyes and Pigments*, 65 (2005) 227
23. E.J. Ruiz, C. Arias, E. Brillas, A. Hernández-Ramírez, J.M. Peralta-Hernández. *Chemosphere*, 82 (2011) 495
24. M. Karatas, Y. Alparslan Argun, M. Emin Argun, *J. Ind. Eng. Chem*, 18 (2012) 1058